

# Multijet production at the LHC: Event shapes, NNLO predictions and $\alpha_s$

Javier Llorente

Formerly ATLAS Coll., (now at CIEMAT CMS)

Madrid, May 10 2023



Centro de Investigaciones  
Energéticas, Medioambientales  
y Tecnológicas



2022-T1/IND-23859

# QCD and the running coupling constant

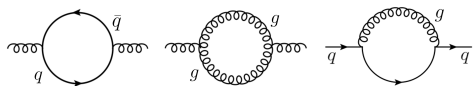
- The QCD coupling  $\alpha_s$  depends on the interaction scale  $Q^2$  through RGE:

$$\frac{\partial \alpha_s}{\partial \log Q^2} = \beta(\alpha_s) = -\alpha_s^2 (\beta_0 + \beta_1 \alpha_s + \beta_2 \alpha_s^2 + \mathcal{O}(\alpha_s^3))$$

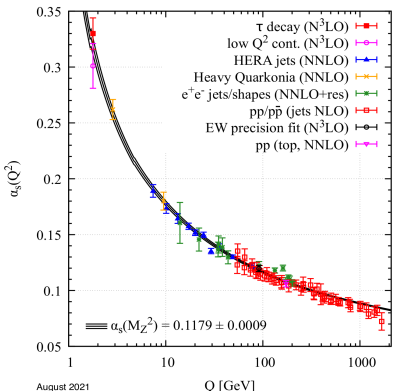
- The solution at three-loop precision reads

$$\frac{\alpha_s}{4\pi}(Q^2) = \frac{1}{\beta_0 x} \left[ 1 - \frac{\beta_1}{\beta_0^2} \frac{\log x}{x} + \frac{\beta_1^2}{\beta_0^4 x^2} \left( \log^2 x - \log x - 1 + \frac{\beta_2 \beta_0}{\beta_1^2} \right) \right]; \quad x = \log \left( \frac{Q^2}{\Lambda^2} \right)$$

Standard Model with  $n_f$  quark flavours:



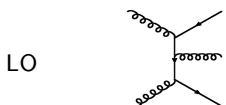
$$\left. \begin{aligned} \beta_0 &= 11 - \frac{2}{3} n_f \\ \beta_1 &= 102 - \frac{38}{3} n_f \\ \beta_2 &= \frac{2857}{2} - \frac{5033}{18} n_f - \frac{325}{54} n_f^2 \end{aligned} \right\}$$



# Fixed order theoretical predictions to three-jet production

- Recently, three-jet cross sections have been calculated at NNLO.
- [M. Czakon *et al.*, arXiv:2106.5331]; [M. Álvarez, *et al.*, arXiv:2301.01086]

$$d\sigma_3 = \sum_{i,j,a,b,c} \int_{\Omega} d^2\vec{x} d^3\vec{z} f_i(x_1, \mu_F^2) f_j(x_2, \mu_F^2) d\hat{\sigma}_{ij \rightarrow abc}(\vec{x}, \mu_R^2) D_a^h(z_3, \mu_f^2) D_b^h(z_4, \mu_f^2) D_c^h(z_5, \mu_f^2)$$

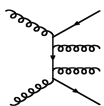


LO

Born  $\mathcal{O}(\alpha_s^3)$

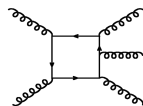
$$\hat{\sigma}_{ij \rightarrow abc} \propto |\mathcal{M}|^2 = \sum_{i,j \in \mathcal{D}} \mathcal{M}_i^* \mathcal{M}_j$$

PDFs from various fits [EPJC 75, 132 (2015)]



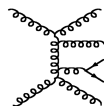
NLO

Real finite  $\mathcal{O}(\alpha_s^4)$

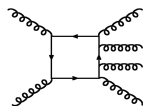


Fragmentation from MC  
[2203.11601], [1512.01178]

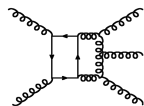
NNLO



Real-real finite  $\mathcal{O}(\alpha_s^5)$



Real-virtual finite  $\mathcal{O}(\alpha_s^6)$



Virtual-virtual finite  $\mathcal{O}(\alpha_s^7)$ .

- Event shapes characterise the isotropy of the energy distribution.
- Two main families are considered: Thrust-based and Sphericity-based.
- Transverse Thrust and Transverse Thrust Minor:

$$\tau_{\perp} = 1 - \frac{\sum_i |\vec{p}_{T,i} \cdot \hat{n}_T|}{\sum_i |\vec{p}_{T,i}|}; \quad T_m = \frac{\sum_i |\vec{p}_{T,i} \times \hat{n}_T|}{\sum_i |\vec{p}_{T,i}|}$$

- The 2 and 3-dimensional Sphericity tensors  $\mathcal{M}_{\alpha\beta} = \frac{1}{\sum_i |\vec{p}_i|} \sum_i \frac{p_i^\alpha p_i^\beta}{|\vec{p}_i|}$ , i.e.

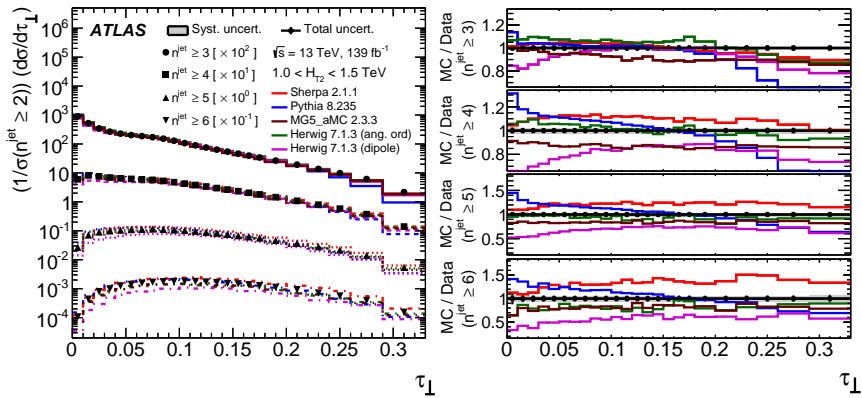
$$\mathcal{M}_2 = \frac{1}{\sum_i |\vec{p}_i|} \sum_i \frac{1}{|\vec{p}_i|} \begin{pmatrix} p_{xi}^2 & p_{xi}p_{yi} \\ p_{yi}p_{xi} & p_{yi}^2 \end{pmatrix} \quad \mu_1 \geq \mu_2; \quad \lambda_1 \geq \lambda_2 \geq \lambda_3$$

$$\mathcal{M}_3 = \frac{1}{\sum_i |\vec{p}_i|} \sum_i \frac{1}{|\vec{p}_i|} \begin{pmatrix} p_{xi}^2 & p_{xi}p_{yi} & p_{xi}p_{zi} \\ p_{yi}p_{xi} & p_{yi}^2 & p_{yi}p_{zi} \\ p_{zi}p_{xi} & p_{zi}p_{yi} & p_{zi}^2 \end{pmatrix}$$

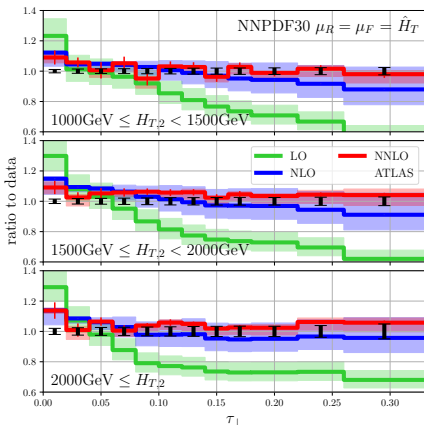
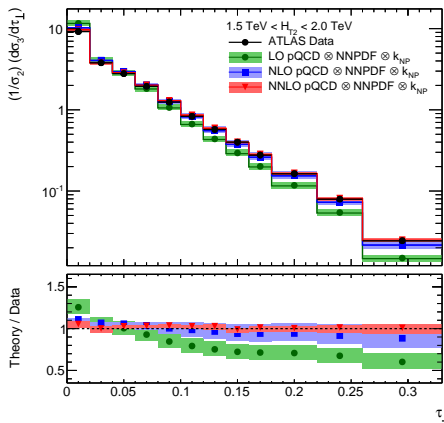
- Transverse Sphericity  $S_{\perp} = \frac{2\mu_2}{\mu_1 + \mu_2}$
- Aplanarity  $A = \frac{3}{2}\lambda_3$
- $C = 3(\lambda_1\lambda_2 + \lambda_1\lambda_3 + \lambda_2\lambda_3)$
- $D = 27\lambda_1\lambda_2\lambda_3$

Eigenvalues  $\mu_i \in \sigma(\mathcal{M}_2)$  and  $\lambda_i \in \sigma(\mathcal{M}_3)$

- For each bin, the distributions are normalised to two-jet cross section  $\sigma_2$ .
- Large jet multiplicities implies more isotropic events.
- No MC model fully describes the data, either in shape or normalisation.
- As expected the description is worse for larger jet multiplicities.



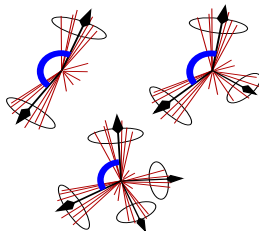
- Each additional perturbative order adds for a better description of  $\tau_{\perp}$ .
- Scale uncertainties reduce with each additional perturbative order.
- NNLO predictions describe the data well, specially for high  $\tau_{\perp}$ .
- Low values of  $\tau_{\perp}$  can be subject to additional resummed corrections.



# Transverse Energy-Energy Correlations in ATLAS [arXiv:2301.09351]

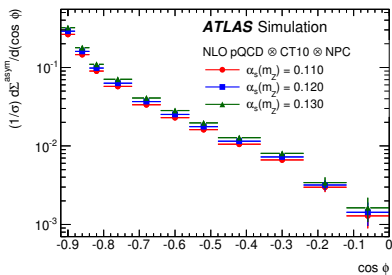
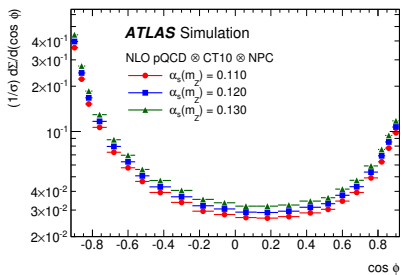
TEEC: The  $x_T$ -weighted distribution of differences in azimuth between jets  $i$  and  $j$ , with  $x_{Ti} = \frac{E_{Ti}}{\sum_k E_{Tk}}$

$$\frac{1}{\sigma} \frac{d\Sigma}{d(\cos \phi)} = \frac{1}{\sigma} \sum_{ij} \int \frac{d\sigma}{dx_{Ti} dx_{Tj} d(\cos \phi)} x_{Ti} x_{Tj} dx_{Ti} dx_{Tj}$$



And the azimuthal asymmetry ATEEC is defined as

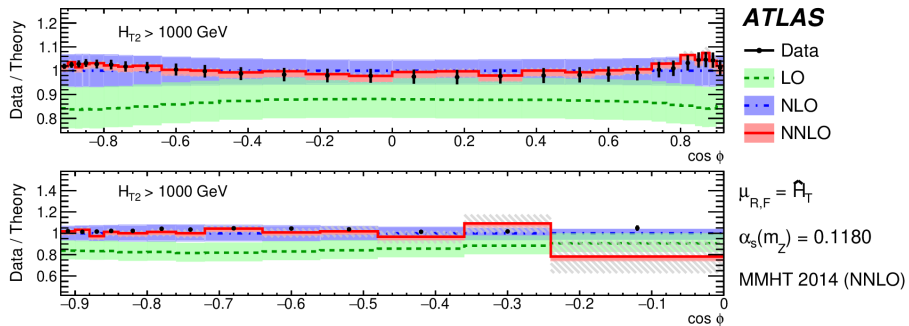
$$\frac{1}{\sigma} \frac{d\Sigma^{\text{asym}}}{d(\cos \phi)} \equiv \left. \frac{1}{\sigma} \frac{d\Sigma}{d(\cos \phi)} \right|_{\phi} - \left. \frac{1}{\sigma} \frac{d\Sigma}{d(\cos \phi)} \right|_{\pi-\phi}$$



ATLAS Collaboration, [[Phys. Lett. B 750, 427 \(2015\)](#)], [[Eur. Phys. J. C 77, 872 \(2017\)](#)]

- Small sensitivity to IR divergences and mild dependence on PDF and  $\mu_R, \mu_F$ .
- Good stability against JES and JER due to  $x_{Ti} x_{Tj}$ -weighting

- Data are compared to theoretical predictions at LO, NLO and NNLO.
- Measurements performed across 10 bins in  $H_{T2}$ , providing 10  $Q^2$  points.
- Intensive use of computing grid (**over 100M CPU hours  $\sim 11K$  years!**)
- Excellent description of collinear and back-to-back regions.
- Important reduction of theoretical uncertainties on QCD scales.



For determining  $\alpha_s(m_Z)$ , a  $\chi^2$  function is minimized in 149+1 dimensions

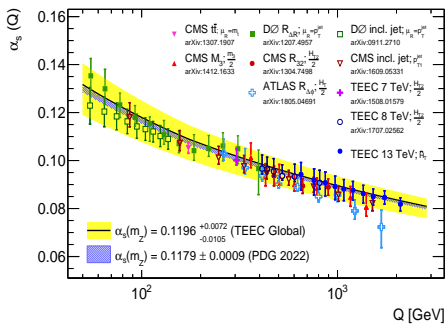
$$\left. \begin{aligned} \chi^2(\alpha_s, \vec{\lambda}) &= \sum_{\text{bins}} \frac{(x_i - F_i(\alpha_s, \vec{\lambda}))^2}{\Delta x_i^2 + \Delta \xi_i^2} + \sum_k \lambda_k^2 \\ F_i(\alpha_s, \vec{\lambda}) &= \psi_i(\alpha_s) \left( 1 + \sum_k \lambda_k \sigma_k^{(i)} \right) \end{aligned} \right\}$$

- $x_i$  is the value of the data distribution in bin  $i$ .
- $\Delta x_i$  and  $\Delta \xi_i$  are the statistical uncertainties for data and theory.
- $\psi_i(\alpha_s) = \sum_{k=0}^3 p_k^{(i)} \alpha_s^k$  parameterises the  $i$ -th bin dependence on  $\alpha_s(m_Z)$ .
- $\sigma_k^{(i)}$  are the relative experimental uncertainties (149 sources).
- $\lambda_k$  are nuisance parameters for each experimental uncertainty.
- Scale uncertainties treated using the offset method:  $\psi_i(\alpha_s)$  is varied.

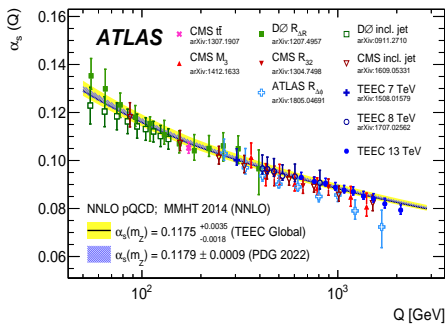
# Transverse Energy-Energy Correlations in ATLAS [arXiv:2301.09351]

- Improves theory uncertainties by a factor of 3 with respect to NLO.
- Good agreement with world average and previous measurements.
- Renormalisation Group Equation probed at the highest scales to date.
- Provides the highest precision points beyond the TeV scale to date.

[ATLAS-CONF-2020-025] (NLO)



[arXiv:2301.09351] (NNLO)

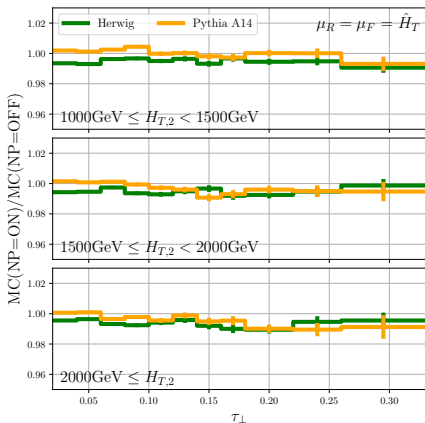
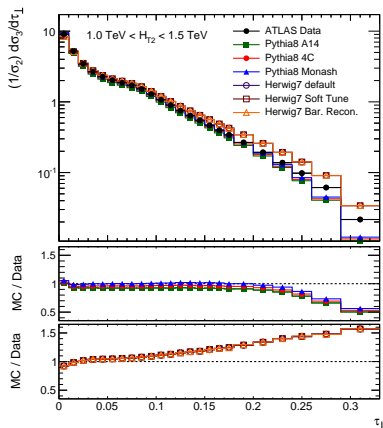


- Event shapes are an interesting way to probe QCD at hadron colliders.
- Experimentally, three-jet event shapes are measured at  $\mathcal{O}(1\%)$  precision.
- Recent theoretical progress allows for a more precise understanding;
  - Improved description of event shapes at the LHC
  - Reduced theoretical uncertainties on  $\mu_R, \mu_F$ .
- Experimentally, event shapes are measured with  $\mathcal{O}(1\%)$  precision.
- This allows for precise determinations of  $\alpha_s(m_Z)$  using TEEC.
- First comparisons of three-jet observables with NNLO predictions.
- Most precise determination of  $\alpha_s(Q)$  over the TeV scale.

# Backup slides

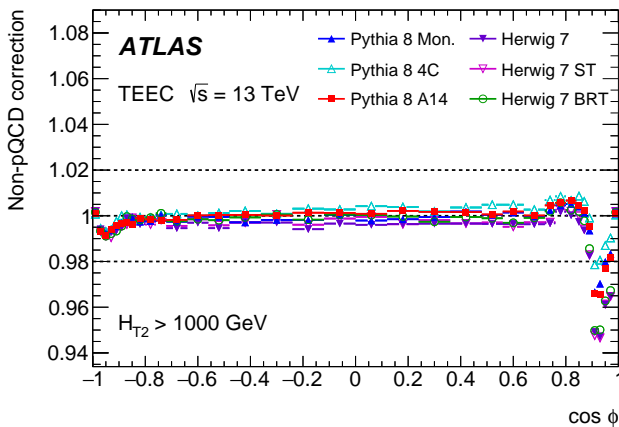
- Non-pQCD corrections cover jet fragmentation and UE effects.
- The effect of these corrections is limited to  $\mathcal{O}(1\%)$  in all regions.
- They are estimated using different MC models and tunes as the ratio

$$C_{NP} = \left( \frac{1}{\sigma_2} \frac{d\sigma_3}{dX} \right)_{UE=ON}^{\text{Had=ON}} \Bigg/ \left( \frac{1}{\sigma_2} \frac{d\sigma_3}{dX} \right)_{UE=OFF}^{\text{Had=OFF}} ; \quad X = \tau_\perp, T_m, A, \dots$$

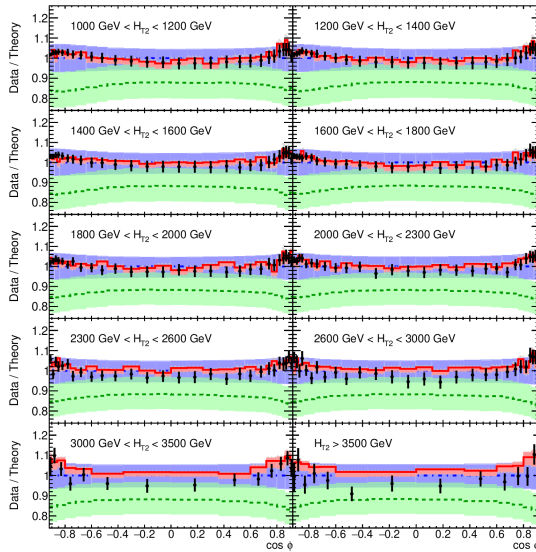


- Non-perturbative corrections obtained in different Pythia / Herwig tunes.
- Mostly unity, with some deviations observed in the collinear region.

$$C_{NP} = \left( \frac{1}{\sigma} \frac{d\Sigma}{d \cos \phi} \right)_{UE=ON}^{\text{Had=ON}} \Bigg/ \left( \frac{1}{\sigma} \frac{d\Sigma}{d \cos \phi} \right)_{UE=OFF}^{\text{Had=OFF}}$$



Good overall description, with theory slightly above the data for high  $H_{T2}$  bins.



**ATLAS**

Particle-level TEEC

$\sqrt{s} = 13 \text{ TeV}; 139 \text{ fb}^{-1}$

$\text{anti-}k_t R = 0.4$

$p_T > 60 \text{ GeV}$

$|\eta| < 2.4$

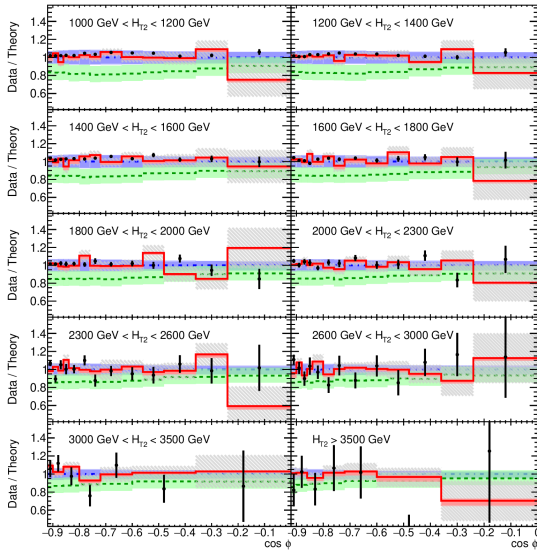
$$\mu_{R,F} = A_T$$

$$\alpha_s(m_Z) = 0.1180$$

MMHT 2014 (NNLO)

- Data
- LO
- NLO
- NNLO

Good overall description, for ATEEC in all  $H_{T2}$  bins.



**ATLAS**

Particle-level ATEEC

$\sqrt{s} = 13 \text{ TeV}; 139 \text{ fb}^{-1}$

$\text{anti-}k_t \text{ R} = 0.4$

$p_T > 60 \text{ GeV}$

$|\eta| < 2.4$

$\mu_{R,F} = \hat{A}_T$

$\alpha_s(m_Z) = 0.1180$

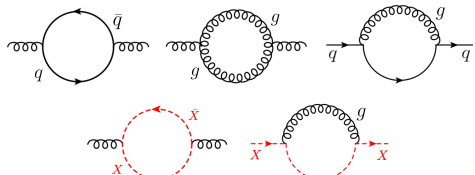
MMHT 2014 (NNLO)

- Data
- LO
- NLO
- NNLO

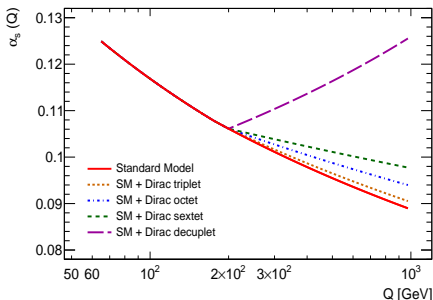
- Testing the running coupling is an important precision test of the SM.
- But also a way to study contributions from new physics beyond the SM!
- New coloured fermions would modify the structure of the  $\beta$  function.

Becciolini et al. [PRD 92, 079905 (2015)]; Llorente, Nachman [NPB 936, 106 (2018)]

Standard Model with  $n_f$  quark flavours +  $n_X$



$$\left. \begin{aligned} \beta_0 &= 11 - \frac{2}{3} n_f - \frac{4}{3} n_X T_X \\ \beta_1 &= 102 - \frac{38}{3} n_f - 20 n_X T_X \left( 1 + \frac{C_X}{5} \right) \end{aligned} \right\}$$



	Triplet	Octet	Sextet	Decuplet
$T_X$	1/2	3	5/2	15/2
$C_X$	4/3	3	10/3	6

# Using the QCD coupling to constrain new physics [NPB 936, 106 (2018)]

- (A)TEEC are calculated at NLO for BSM models.
- A scan is performed over  $m_X$  and  $n_{\text{eff}} = 2n_X T_X$ .
- Likelihood  $L$  is built using the covariance matrix  $V$ .

$$\log L(X, \theta) = -\frac{1}{2}(X - \theta)^T V^{-1}(X - \theta)$$

- Models with  $p$ -value below 0.05 are excluded.

